BIOENG

Brazilian Journal of Biosystems Engineering (2025), 19 1293

REGULAR ARTICLE

Contribution to the mechanical performance of a simply supported lightweight concrete beam reinforced with bio-sourced nanocomposites

Hafid Khetir[1], Abdelmoutalib Benfrid[1], Mohamed Bachir Boiuladjra[1,2]*, Lakhder Melati[1]

[1]Laboratory of Advanced Structures and Materials in Civil Engineering and Public Works, Sidi Bel Abbes, Algeria.
[2]Thematic Agency for Research in Science and Technology (ATRST), Algiers, Algeria.

Regular Section
Academic Editor: Celso Antonio Goulart

Statements and Declarations

Data availability
All data will be shared on request.

Institutional Review Board Statement
Not applicable.

Conflicts of interest
The authors declare no conflict of interest.

Funding
This research did not receive any specific grant from funding agencies in the public, commercial, or non-profit sectors.

Autor contribution
ML: Literature Review; Manuscript Writing; Experimental Data Collection; Manuscript Revision; BA: Conceptualization; Manuscript Writing; CM: Manuscript Revision; HR: Supervision; BB: Experimental Data; Data Storage; Supervision.

Abstract

Gypsum is an essential building material widely used in the construction industry, particularly in the form of lightweight concrete. Nanotechnology has facilitated the enhancement of its properties in recent years by incorporating nanostructured materials from biological sources, such as nanoparticles derived from cow bones and African and Brazilian reeds, known for their superior mechanical properties. This study explores ways to improve the mechanical properties of lightweight concrete composites using nanoparticles from plants or animals. The goal is to enhance the bending performance of lightweight gypsum beams while aiming to reduce production costs by utilizing bio-sourced materials. We used the Mori-Tanaka method to examine the effectiveness of mixing lightweight concrete with nanometric additions from biological sources. The study of beam behavior depends on methods used in continuum mechanics, particularly bending analysis. The beams studied are simply supported. The results show that nanoparticles from bovine bones, African reed, or Brazilian reed not only strengthen the material but also significantly improve the bending performance of lightweight gypsum beams when subjected to bending.

Keywords

Bending Beam Simple Supported; Nano-bio-inclusions; Mori-Tanaka Methodology; Mechanics of Continuous Media.

Introduction

Gypsum is a building material that has been around for a long time and is still useful today. It is often used in architecture, civil engineering, and building. Recently, researchers have focused on improving this material by adding nanoparticles, which will improve its mechanical and thermal properties.

Many studies have been done to find ways to make concrete stronger by adding tiny minerals to the concrete matrix. In 2018, Benkabou et al. introduced a numerical homogenization technique at the nanometric scale to predict the elasto-viscoplastic properties of high-performance concrete (HPC). Their method combines finite element models with nanoindentation tests. You can homogenize things in two ways: by hand and with computers. The numbers match the experimental data very closely, indicating that the method is accurate. (Harrat et al., 2020) Looked at the static properties of concrete beams that had SiO_2 added to them.

Voigt homogenization, which is used to separate the beam corners, makes the mechanical properties better at the nanometric scale. We looked at the beam analytically using higher-order shear deformation theory on a Pasternak-Winkler elastic foundation. The results show that the stresses and deformations have gone down, which shows how much the foundation affects how the structure bends. (2021) Chatbi and others Looked into how silica nanoparticles change the strength of concrete slabs when they are not moving. Using the advanced Voigt model, they showed the best way to mix SiO_2 into the slab while also considering how it separates inside.

According to the study, the slabs are stronger, and the elastic base has a big effect on how they bend. (Benfrid et al., 2023) We looked at how adding nano-glass powder particles to concrete that was put under heat and stress changed it. The study used the Eshelby model to mix concrete and glass nanoparticles and then looked at reinforced concrete panels in a scientific way. It found that nano-glass makes the thermal loads on these panels worse. (Kecir et al., 2024) Used a non-local Eringen modeling method to look at how Fe_2O_3 nanoparticles affect the bending strength of concrete slabs. The study showed that a 30% Fe_2O_3 composition improves the elastic properties by 60% and reduces the deflection of thin plates. This shows that it could be used to strengthen concrete structures. The Eshelby model was used to make things more uniform.

This gives much information about research that has been done on reinforcement using bio-based alternatives. (Emmanuel Georges Lissouck MBEI et al., 2015) Made a composite material that combines plaster with plant fibers from the rainforest in South Cameroon. Ultrasonic testing showed that the material was not uniform, and with the proper calibration settings, the longitudinal wave velocity was 6217 m/s. These results can be used to add waviness or sinuous

*Corresponding authors
E-mail address: mohamedbachirbouiadjra@gmail.com

https://doi.org/10.18011/bioeng.2025.v19.1293
Received:10 July 2025 / Accepted: 04 December 2025 / Available online: 18 February 2026

elements to codes for structural design. (Beli NEYA et al., 2018) Researchers in Burkina Faso made a composite material out of plaster, sand, and Kenaf fibers to make it more flexible and better at keeping heat.

Adding 1% Kenaf fibers does not change the thermal conductivity much, but it does make the material stronger and change how it breaks. When looked at under a microscope, the fibers are evenly spread out along the whole length of the samples. (Betene Ebanda et al., 2018) This study looks at how Rhecktophyllum camerunense fibers absorb water by looking at how they diffuse at three different levels of relative humidity (23%, 54%, and 75%) at 23±1°C. Results show that adsorption happens quickly at first, reaching saturation by the seventh hour. The maximum moisture content rises as relative humidity rises. The data fit Fick's Law, which says that the diffusion coefficient goes up in a straight line as relative humidity goes up. (Noutegomo Boris et al., 2023) This study looks at the hydromechanical properties of Rhecktophyllum camerunense (RC) fibers, which are used as environmentally friendly substitutes for glass fibers in composite materials.

The fibers were put through different levels of humidity and soaked in distilled water. This lowers the stress at break and elastic modulus, but the toughness and significant elongation at break stay the same. The results show how important pre-treatment is for making fibers work better in composite materials. (Benfrid et Bachir Bouiadjra, 2025) Look into how adding natural fibers to plaster (gypsum) can make it stronger They make a mathematical model to see how biological beams bend by using Piggot's rule for homogenization. The results show that the deflection has gone down a lot and the shear strength has gone up. This supports the use of building materials that are good for the environment and last a long time.

Recent scientific studies have investigated static bending analyses that use the continuous media approach. (L. Hadji et al., 2015) This study shows a better way to use the exponential shear deformation theory to look at how functionally graded beams bend. It includes parabolic changes in transverse shear strain and considers the stretching effect. People think that the properties of materials follow a power law distribution. We can find analytical solutions for static bending, and numerical examples show that the theory is right. (S. M. Ghumare et al., 2017) This paper talks about a new theory called fifth-order shear and standard deformation theory (FOSNDT) that can be used to study static bending and elastic buckling in functionally graded beams, where the material properties change in a power-law pattern over the thickness. The theory uses polynomial shape functions of up to fifth order to account for both typical deformations and transverse shear.

This means that it can make accurate predictions without having to use shear correction factors. Navier's solution shows that the theory is more accurate and useful than classical and higher-order shear deformation theories. (M Chitour et al., 2024) Using a cutting-edge 2D shear deformation theory, see how supported functionally graded material beams act when they aren't moving. This theory says that Young's modulus changes based on a power-law distribution that depends on how much of each material is present. We use the idea of virtual work to write the equilibrium equations and Navier's solution for sandwich beams to solve them mathematically.

The study uses both comparative and parametric studies to test the theory's accuracy and see how beams act when different things are changed, like the type of beam, the material index, the thickness ratio, and the boundary conditions. (Dang Diem Nguyen et al., 2025) The stochastic finite element method (SFEM) is what this paper is about. It is used to find the static response of beams with an elastic modulus that changes in two dimensions. The method uses a two-dimensional random field to show how different materials are and first-order perturbation methods to find the statistical moments of displacement. The results are very similar to those from Monte Carlo simulations, and they show how the coefficient of variation (COV) of displacement changes with the correlation length. The Mori-Tanaka homogenization method was used in this study to find out what the mechanical properties of a matrix with spherical nano-inclusions were. (Mori-Tanaka, 1973) It is used to find the modulus of a matrix that has inclusions. This is common with materials like mortar, where the paste serves as both the matrix and the inclusion. In this case, the plaster is the matrix and the nanoparticles made from cow or reed bones are the nano-inclusions.

You need to know a lot of important things to do this, like the volume fraction based on the material's nano-composition and mechanical properties. (1975; Rho et al., 1997; Currey, 2012) Several studies and experiments have found that the elastic modulus of cow bones is probably between 17 GPa and 22 GPa. There are two types of African and Australian reeds: (Luisa Molari et al., 2021; Lorenzo et al., 2019; Ghavami, 1995) When dry, the Young's modulus of Arundo donax (giant reed) is 10 to 12 GPa, and the elasticity of Phragmites australis (common reed) is 3 to 8 GPa. Studies (Lakkad & Patel, 1981; Janssen, 2000; Yalçin et al., 2022) also show that African bamboo, Oxytenanthera Abyssinia, has a modulus of 20 GPa, and Brazilian bamboo has a modulus of 17 to 25 GPa. This study is all about the matrix. (Zivica, 2002; Krzysztof Powała et al., 2022) This means that the elastic modulus of building gypsum is 5 GPa.

The next part is an analysis of static bending using the continuous media mechanics approach after homogenization. The results show that nano-reinforcements make things work better mechanically, while deflection decreases as the concentration of nano-inclusions increases.

Materials and methods

Homogenization by Mori-Tanaka: The Mori-Tanaka model is used to figure out the modulus of a matrix that has nano-spheres as nano-inclusions. It is beneficial for materials like gypsum, where the gypsum is the matrix and the bio-sourced material is the nano-inclusions.

One unit is the volume of plaster plus the volume of bio-sourced reinforcement.

$$V_m = 1 - V_c \quad \textbf{(1)}$$

The compressibility modulus, shear modulus, Young's modulus, and Poisson's ratio all affect each other. These relationships are used to figure out the material's compressibility and shear coefficients. The material is made of plaster and spherical bio-sourced nano-inclusions.

$$K_m = \frac{E_m}{3(1-2\nu_m)}, \quad K_c = \frac{E_c}{3(1-2\nu_c)}, \quad G_m = \frac{E_m}{3(1+2\nu_m)}, \quad G_c = \frac{E_m}{2(1+\nu_c)} \tag{2}$$

The effective bulk modulus (compressibility) (k) and shear modulus (G) are expressed as follows:

$$\frac{K-K_m}{K_C-K_m} = \frac{V_c}{1+V_m\left(\frac{K_c-K_m}{K_m+\frac{4}{3}G_m}\right)} \tag{3}$$

$$\frac{G-G_m}{G_C-G_m} = \frac{V_c}{1+V_m\left(\frac{G_c-G_m}{G_m+f1}\right)} \tag{4}$$

Where:

$$f_1 = \frac{G_m(9K_m+8G_m)}{6(K_m+2G_m)} \tag{5}$$

The effective modulus of elasticity E and Poisson's ratio ν are determined using the relation:

$$E = \frac{9KG}{3K+G}, \quad \nu = \frac{3K-2G}{2(3K+G)} \tag{6}$$

It is noted that:

E: Homogeneous Elasticity Modulus (Plaster + Bio-sourced reinforcement nano-inclusions).

K: Homogeneous Compressibility Modulus (Plaster + Bio-sourced reinforcement nano-inclusions).

G: Homogeneous Shear Modulus (Plaster + Bio-sourced reinforcement nano-inclusions).

E_m: Matrix Elasticity Modulus (Plaster).

E_c: Composite Elasticity Modulus (Bio-sourced reinforcement nano-inclusions).

K_m: Matrix Compressibility Modulus (Plaster).

K_c: Composite Compressibility Modulus (Bio-sourced reinforcement nano-inclusions).

G_m: Matrix Shear Modulus (Plaster).

G_c: Composite Shear Modulus (Bio-sourced reinforcement nano-inclusions).

V_m: Matrix Volume (Plaster).

V_c: Composite Volume (Bio-sourced reinforcement nano-inclusions).

ν_m: Matrix Poisson's Ratio (Plaster).

ν_c: Composite Poisson's Ratio (Bio-sourced reinforcement nano-inclusions).

Analytical Model of Static Bending: The displacement field is written in the form of the refined theory.

$$u_1(x,z,t) = u(x,z,t) - z\frac{dw_b}{dx} - f(z)\frac{dw_s}{dx}; \quad u_2(x,z,t) = 0; \quad u_3(x,y,z_{ns},t) = w_b(x,t) + w_s(x,t) \tag{7}$$

The deformation and distortion are defined as: follows:

$$\varepsilon_x = \frac{du}{dx} + z\frac{\partial^2 w_b}{\partial x^2} - f\frac{\partial^2 w_s}{\partial x^2}; \quad \gamma_{xz} = \left(1-\frac{df}{dz}\right)\frac{dw_s}{dx} = g\frac{dw_s}{dx} \tag{8}$$

Noted that: used by (Benfrid et Bachir Bouiadjra, 2025).

$$f(z) = \frac{3}{8}z + \frac{41}{30}\frac{z^3}{h^2} - 0.5h\arctan\left(\frac{\pi z}{h}\right) \tag{9}$$

Where:

$$g = 1 - \frac{df}{dz} \tag{10}$$

The equations of motion with virtual principal simplify

$$\int_{-h/2}^{h/2}\int_{\Omega}\left[\sigma_x\delta\varepsilon_x + \tau_{xz}\delta\gamma_{xz}\right]d\Omega w dz - \int_{\Omega} q\,\delta w d\Omega = 0 \tag{11}$$

The variation of deformation is defined as follows:

$$\delta U = \int_0^L\int_A(\sigma_x\delta\varepsilon_x + \tau_{xz}\delta\gamma_{xz})dAdx = \int_0^L\left(N\frac{d\delta_u}{dx} - M_b\frac{d^2\delta w_b}{dx^2} - M_s\frac{d^2\delta w_s}{dx^2} + Q\frac{d\delta w_s}{dx}\right)dx \tag{12}$$

The variance of the potential

$$\delta V = -\int_0^L q\,\delta(w_b + w_s)dx \tag{12}$$

The resultant forces, moments, and shear forces are designated as follows:

$$N = \int_A \sigma_x dA; \quad N_b = \int_A z\sigma_x dA; \quad M_S = \int_A f(z)\sigma_x dA; \quad Q = \int_A g(z)\tau_{xz}dA \tag{13}$$

By replacing (13) in (11) the equilibrium equations are written:

$$\delta u : \frac{dN}{dx} = 0 \quad (14)$$
$$\delta w_b : \frac{d^2 M_b}{dx^2} + q = 0$$
$$\delta w_s : \frac{d^2 M_s}{dx^2} + \frac{dQ}{dx} + q = 0$$

The boundary conditions

$$w_b \, or Q_b = \frac{dM_b}{dx} \quad (15)$$
$$w_s \, or Q_s = \frac{dM_s}{dx} + Q$$
$$\frac{dM_b}{dx} \, or M_b$$
$$\frac{dM_s}{dx} \, or M_s$$

The relationship between constraint and deformation is defined as follows:

$$\sigma_x = Q_{11}\varepsilon_x \; ; \; \tau_{xz} = Q_{55}\gamma_{xz} \quad (16)$$

Where:(For isotropic materials)

$$Q_{11} = E \quad (17)$$

$$Q_{55} = \frac{E}{2} + [1 + \nu]$$

By substituting:

$$N = A\frac{du}{dx} - B\frac{d^2 w_b}{dx^2} - B_s \frac{d^2 w_s}{dx^2} \quad (18)$$
$$M_b = B\frac{du}{dx} - D\frac{d^2 w_b}{dx^2} - D_s \frac{d^2 w_s}{dx^2} \quad ;$$

$$M_s = B_s \frac{du}{dx} - D_s \frac{d^2 w_b}{dx^2} - H_s \frac{d^2 w_s}{dx^2} \quad (19)$$
$$Q = A_s \frac{dw_s}{dx} \quad ;$$

With:

$$A = \int_A Q_{11} dA \quad B = \int_A z Q_{11} dA \quad B_s = \int_A f(z) Q_{11} dA \quad ; \quad ; \quad ; \quad (20)$$
$$D = \int_A z^2 f(z) Q_{11} dA$$

$$D_s = \int_A z \; f(z) Q_{11} dA \quad H_s = \int_A f^2(z) Q_{11} dA \quad ; \quad ; \quad (21)$$
$$A_s = \int_A g^2(z) Q_{55} dA$$

Equation of motion:

$$D_s = \int_A z \; f(z) Q_{11} dA \quad H_s = \int_A f^2(z) Q_{11} dA \quad ; \quad ; \quad (22)$$
$$A_s = \int_A g^2(z) Q_{55} dA$$

$$B\frac{d^3 u}{dx^3} - D_s \frac{d^4 w_b}{dx^4} - H_s \frac{d^4 w_s}{dx^4} + A_s \frac{d^2 w_s}{dx^2} + q = 0 \quad (23)$$

Analytical solution (Navier):

$$u(x,t) = \sum_{n=1}^{\infty} U_n \cos(\alpha x) \quad ; \quad (24)$$
$$w_b(x,t) = \sum_{n=1}^{\infty} W_{bn} \sin(\alpha x) \quad ;$$
$$w_s(x,t) = \sum_{n=1}^{\infty} w_{sn} \sin(\alpha x)$$

Where:

$$\alpha = \frac{n\pi}{L}, (U_n, W_{bn}, W_{sn}) \quad (25)$$

Used Fourier series:

$$q(x) = \sum_{n=1}^{\infty} Q_n \sin(\alpha x) \quad (26)$$

Where load amplitude noted by:

$$Q_n = \frac{2}{L}\int_0^L q(x)\sin(\alpha x)dx \quad (27)$$

The coefficients Qn are given calculated from: (for uniform Loading)

$$Q_n = \frac{4q_0}{n\pi}(n = 1,3,5,....) \quad (28)$$

By replacing (20 to 24) and (25 to 29) in (07) for two directions in loads the stiffness matrix noted:

$$\begin{bmatrix} S_{11} & S_{12} & S_{13} \\ S_{21} & S_{22} & S_{23} \\ S_{13} & S_{23} & S_{33} \end{bmatrix} \begin{Bmatrix} U_n \\ W_{bn} \\ W_{sn} \end{Bmatrix} = \begin{Bmatrix} 0 \\ Q_n \\ Q_{sn} \end{Bmatrix} \quad (29)$$

$$S_{11} = A\alpha^2, \; S_{12} = B\alpha^3, \; S_{13} = B_s\alpha^3, \; S_{22} = D\alpha^4, \quad (30)$$
$$S_{23} = D_s\alpha^4, \; S_{33} = H_s\alpha^4 + A_s\alpha^2$$

The dimensional parameters are written in this formula:

$$\overline{w} = 100\frac{E_m h^3}{q_0 L^4} w\left(\frac{L}{2}\right) \quad , \quad \overline{u} = 100\frac{E_m h^3}{q_0 L^4} u\left(0, -\frac{h}{2}\right) \qquad (31)$$

$$\overline{\sigma_x} = \frac{h}{q_0 L}\sigma_x\left(\frac{L}{2}, \frac{h}{2}\right) \overline{\tau_{xz}} = \frac{h}{q_0 L}\sigma_{xz}(0,0)$$

Results and discussion

Figure 1 shows how the Mori-Tanaka method is used to make a periodic medium more uniform, which leads to an isotropic material through this analytical model.

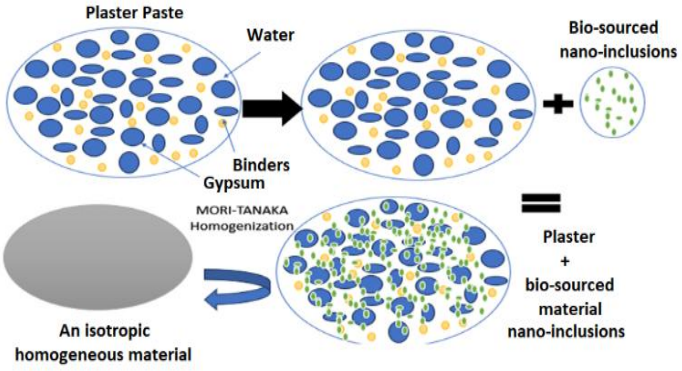

Figure 1. The homogenization process using the Mori-Tanaka method.

Table 1 presents the mechanical properties of the matrix (gypsum) and the nano-reinforcements (reed and bovine bones). The value of Poisson's ratio "v" is always 0.2.

Table 1. The elasticity modulus (E) and Poisson's ratio (v) of the matrix and the nano-reinforcements.

Materials matrix and reinforcements	The Elastic Modulus (GPa) "E"	Poisson's Ratio "v"	Symbols
Gypsum	5	0.2	Gyps
Dry bovine bones	22	0.2	DBB
Arundo donax (giant reed)	12	0.2	ADGR
Phragmites australis (common reed)	8	0.2	PACR
African bamboo (*Oxytenanthera abyssinica*)	20	0.2	ABOA
Brazilian bamboo (*Guadua angustifolia*)	25	0.2	BBGA

Table 2 shows that adding bio-based nano-inclusions to plaster causes the elastic modulus "E" to rise significantly. The formulation with nano-BBGA performs the best, reaching 7.500 GPa at a 30% volume fraction, which is 50% higher than the baseline value of 5 GPa. Nano-DBB shows a significant improvement, reaching 7.329 GPa at 30% Vf, which is a 46.58% increase. On the other hand, nano-PACR shows a more gradual rise, with the elastic modulus reaching 7.195 GPa at 30% Vf. This means that nano-BBGA makes things stiffer and more resistant to deformation the most, but nano-DBB also plays a big part. Nano-PACR works, but it does not work as well as other options. Table 3 shows that the compressibility modulus "K" goes up when nano-inclusions are added, which means that the material is more resistant to compression. The formulation with nano-BBGA shows the most significant improvement, reaching 4.167 GPa at a 30% volume fraction, which is a 50% increase from the original value. Nano-DBB shows a significant rise, reaching 4.072 GPa at 30% Vf, which means it has improved by 46.47%. The compressibility modulus of the nano-PACR formulation rises more steadily, reaching 3.997 GPa at 30% Vf. This means that nano-BBGA gives the most significant boost to compressibility, while nano-DBB is a good alternative. Nano-PACR, on the other hand, only makes a slight difference. As shown in Table 4, adding nano-inclusions to the material increases the shear modulus "G," but the changes are not as significant as those seen in the elastic and compressibility moduli. The formulation with nano-DBB has the highest shear modulus, reaching 3.015 GPa at a volume fraction of 30%. The nano-BBGA formulation, on the other hand, shows a drop in shear modulus at 30% Vf, down to 2.125 GPa. This suggests that nano-BBGA greatly increases stiffness and compressibility, but it may lower shear resistance at high concentrations. Nano-PACR steadily rises, reaching 2.998 GPa at 30% Vf, which is still very high and shows that it works to improve shear resistance.

Table 2. The elastic modulus "E" for various plaster types reinforced with nano-bio-inclusions as a function of volume fractions "Vf".

Volume fractions "V_f" In (%)	The elastic modulus "E" (GPa)				
	Gyps + DBB	Gyps + ADGR	Gyps + PACR	Gyps + ABOA	Gyps + BBGA
00%	5	5	5	5	5
10%	5.672	5.429	5.236	5.633	5.712
20%	6.441	5.897	5.484	6.364	6.538
30%	7.329	6.409	5.738	7.195	7.500

Table 3. The compressibility modulus "K" for various plaster types reinforced with nano-bio-inclusions as a function of volume fractions "Vf".

Volume fractions "V_f" In (%)	The compressibility modulus "K" (GPa^{-1})				
	Gyps + DBB	Gyps + ADGR	Gyps + PACR	Gyps + ABOA	Gyps + BBGA
00%	2.778	2.778	2.778	2.778	2.778
10%	3.151	3.016	2.909	3.132	3.175
20%	3.578	3.276	3.047	3.575	3.632
30%	4.072	3.561	3.191	3.997	4.167

Table 4. Shear modulus "G" for various plaster types reinforced with nano-bio-inclusions as a function of volume fractions "Vf".

Volume fractions "V_f" In (%)	The compressibility modulus "K" (Gpa)				
	Gyps + DBB	Gyps + ADGR	Gyps + PACR	Gyps + ABOA	Gyps + BBGA
00%	2.083	2.083	2.083	2.083	2.083
10%	2.263	2.262	2.182	2.249	2.381
20%	2.684	2.457	2.285	2.651	2.724
30%	3.015	2.671	2.393	2.998	2.125

It is always necessary to validate a calculation program through previous studies or comparisons with other recent results in the scientific research literature. To check the way the calculation is done in the static bending section, it is best to use a functionally graded material (FGM) beam, as shown in (L. Hadji et al., 2015) and (M. Chitour et al., 2024). The beam should have an "Em = 70 GPa" (aluminum) and "Ec = 380 GPa" (ceramic) and a Poisson's ratio of v = 0.3. Setting the homogenization power P to 0 is enough to compare the results. It is interesting to note that the function used in this study has also been used by Benfrid and Bachir Bouiadjra (2025) and that the results are very close to what we expected, which shows that our computational programming is accurate.

Table 5 clearly shows the differences between transverse displacement, deflection, everyday stress, and tangential stress for the geometric parameters "a=5h" and "a=20h" using two methods: (L. Hadji et al., 2015), (M. Chitour et al., 2024), and the current research. The results for transverse displacement and deflection are very similar across the different methods. The values of this study are very similar to those of (L. Hadji et al., 2015) and (M. Chitour et al., 2024), which means they agree strongly. The normal stress values are very similar, and the results from the current method are almost the same as those from the other two studies. The values for tangential stress are mostly the same, with only small differences at "a=5h" and "a=20h." The results of this study are very similar to those of established methods. This shows that the method used by Benfrid and Bachir Bouiadjra (2025) is accurate and reliable.

Table 5. The transverse displacement, deflection, normal stress, and tangential stress are examined for the geometric parameter "a=5h or a=20h".

Method	a=5h				a=20h			
	$\bar{u}$	$\bar{w}$	$\bar{\sigma}_x$	$\bar{\tau}_{xz}$	$\bar{u}$	$\bar{w}$	$\bar{\sigma}_x$	$\bar{\tau}_{xz}$
(L. Hadji et al., 2015)	0.9233	3.1673	3.9129	0.7883	0.2290	2.8807	15.4891	0.7890
(M Chitour et al., 2024)	0.9375	3.1643	3.7954	0.7333	0.2305	2.8962	15.0112	0.7455
Present*	0.9256	3.1674	3.7772	0.7681	0.2272	2.9082	15.4995	0.7694

Figure 2 illustrates the lateral displacement behavior of standard beams and beams reinforced with different nano-bio inclusions at concentrations of 10%, 20%, and 30%. The analysis reveals notable differences between the untreated (standard) beams and those with added nanoparticles. The standard beams exhibit the greatest transverse displacements, indicating they are less stiff and bend more when subjected to loading. In contrast, the addition of nanoparticles significantly reduces these displacements, improving the overall bending performance of the structure.

Adding Nano-DBB to the beams results in reduced lateral movement at all concentrations. At 10%, the displacements are already much lower than those of the standard beam, and at 20% and 30%, this reduction becomes even more pronounced. As the concentration of Nano-DBB increases, the beams become progressively stiffer. The 30% concentration has the most substantial impact, significantly reducing lateral displacements. This indicates that Nano-DBB improves the material's stability, making the beam stronger and less prone to bending under stress.

Beams reinforced with Nano-ADGR show a slight increase in transverse displacements. While the reduction at 10% is not as significant as with Nano-DBB, it still represents an important improvement. At 20% and 30%, the displacements continue to decrease, but the reduction is less marked than with Nano-DBB. This suggests that Nano-ADGR enhances the beam's performance, but its effect is less pronounced, possibly due to weaker interactions with the gypsum matrix.

Beams with Nano-PACR show minimal changes in lateral displacements. At 10%, there is a small improvement, which increases at 20% and 30%, but still remains inferior to the performance of Nano-DBB or Nano-ADGR. This indicates that while Nano-PACR provides some reinforcement, it does not significantly affect rigidity or deflection.

Beams reinforced with Nano-ABOA and Nano-BBGA show only minor changes in their lateral movement. At 10%, both nanoparticles provide small improvements, but the improvements diminish further at 20% and 30%. This suggests that these nanoparticles are less effective in enhancing the beams' strength. Nano-ABOA, in particular, shows only a marginal difference, especially at 30%, indicating that it does not significantly increase beam stiffness when interacting with the gypsum matrix.

In conclusion, adding nano-bio inclusions at concentrations of 10%, 20%, and 30% significantly improves beam performance by reducing transverse displacements. Nano-DBB is the most effective nanoparticle, particularly at 30%, in minimizing lateral displacements. While Nano-ADGR, Nano-PACR, Nano-ABOA, and Nano-BBGA also help reduce displacements, they are not as effective as Nano-DBB. Nano-DBB consistently outperforms the others in enhancing rigidity and minimizing deformation.

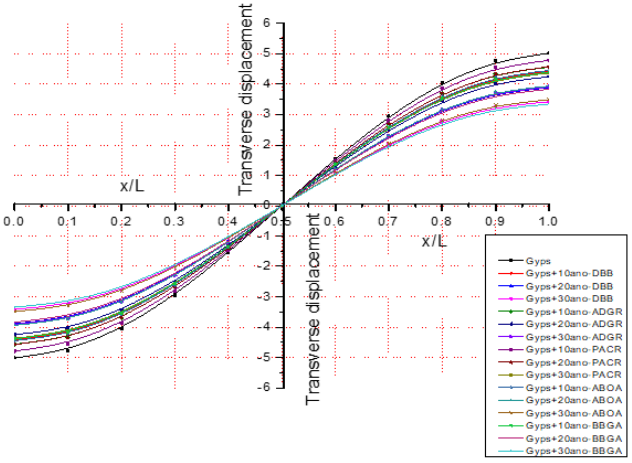

Figure 2. Transverse displacements in various beam types (conventional and reinforced with nano-bio-inclusions).

Figure 3 presents the results of the deflection analysis for two types of beams: standard gypsum beams and beams reinforced with nanoparticles. The nanoparticle-reinforced beams show a significant reduction in deflection compared to pure gypsum, with improvements becoming more pronounced at concentrations of 20% and 30%. Adding nanoparticles increases the stiffness of the material, which results in less bending at higher concentrations. Among the nanoparticles tested, Nano-DBB stands out due to its positive effect, reducing deflection even at concentrations as low as 10%. This makes it the best choice for strengthening gypsum.

At a 10% nanoparticle concentration, the reduction in deflection is not as substantial as at higher concentrations, but it still represents a significant improvement over pure gypsum.

At this lower concentration, Nano-DBB proves to be more effective, offering a cost-efficient solution while also enhancing material performance. Nanoparticle-reinforced composites perform better in bending compared to pure gypsum, making them more suitable for applications that require greater stability and durability. It is important to note that excessive nanoparticle concentrations can cause agglomeration, reducing their effectiveness. Therefore, it is crucial to use the optimal amount of nanoparticles to achieve the maximum benefits with minimal negative effects. In conclusion, adding nanoparticles to gypsum strengthens construction materials, making them more resistant to bending or breaking under mechanical loads, which ultimately enhances the longevity of structures.

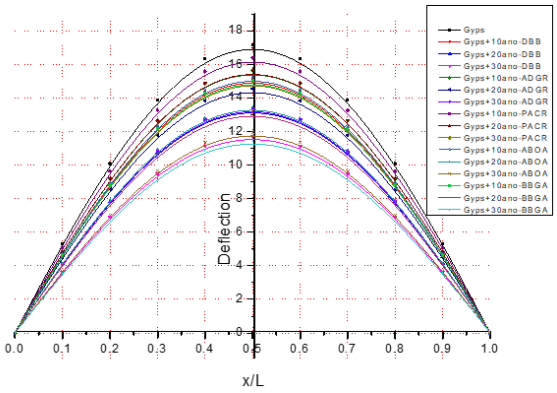

Figure 3. Deflection in different types of beams (ordinary and reinforced with nano-bio-inclusions) (Authors)

Figure 4 shows the normal stress distribution along the x-axis for beams under bending. These beams experience both compressive and tensile stresses. The negative values, ranging from -3.93764 to -0.7487, indicate that the beam is under compressive stress on its inner side. The positive values, ranging from 0.7487 to 3.93764, indicate that the beam is under tensile stress on its outer side. This symmetrical stress distribution is characteristic of bending behavior. The maximum stress occurs at the outermost fibers of the beam and decreases progressively as it moves toward the neutral axis, where the stress is zero. The addition of nano-bio materials appears to alter how stress is distributed, potentially making the beam stiffer and giving it a more uniform stress profile. This could improve its overall mechanical properties.

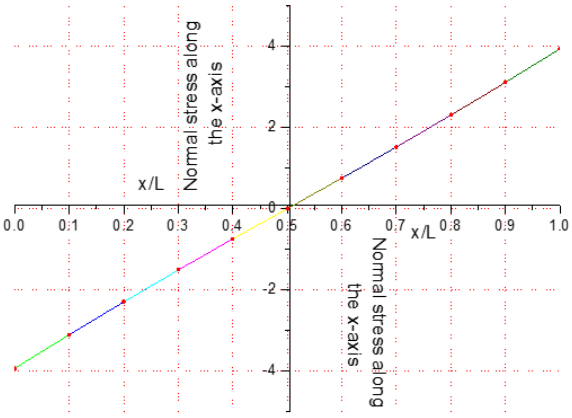

Figure 4. Normal Stress Along the x-axis for Different Types of Beams Reinforced with Nano-Bio Inclusions.

Figure 5 illustrates the distribution of tangential stress (x-z) for different types of beams with nano-bio inclusions. The analysis reveals that the tangential stress follows a parabolic distribution across the beam, ranging from -h/2 to h/2, with the highest stress occurring at the neutral axis (h=0). This distribution reflects bending stress, where the stress is maximal at the neutral axis and gradually decreases toward the outer surfaces of the beam. The tangential stress reaches a peak at the center and then decreases in proportion to the distance from the neutral axis, forming a parabolic curve. This behavior aligns with traditional beam theory, which predicts that shear stress is highest at the neutral axis and lowest at the beam's edges. The addition of various nano-bio materials (Nano-DBB, Nano-ADGR, Nano-PACR, Nano-ABOA, and Nano-BBGA) is expected to alter the stress distribution, potentially improving the beam's mechanical properties and enhancing its performance compared to beams made solely from gypsum.

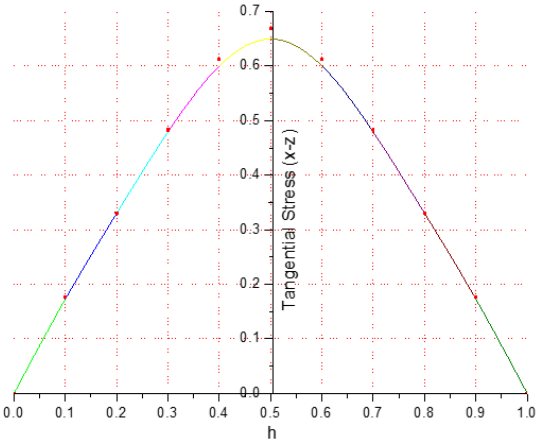

Figure 5. Tangential Stress (x-z) for Different Types of Beams Reinforced with Nano-Bio Inclusions. (Authors)

Conclusions

In conclusion, incorporating bio-based nano-inclusions into gypsum significantly enhances its mechanical properties, particularly in terms of stiffness and compressive strength. Among the formulations studied, Nano-BBGA shows the most significant improvements in performance, although its effect on shear resistance diminishes at higher concentrations. Nano-BBGA and Nano-DBB are best suited for applications requiring strong resistance, while Nano-PACR provides more moderate improvements. Nanoparticles help reduce transverse displacements, which enhances the stiffness and bending resistance of gypsum beams, with higher concentrations leading to greater improvements.

Nano-DBB, especially at concentrations of 20% and 30%, causes the most significant reduction in displacements. In contrast, Nano-ADGR results in only a slight increase in performance, while Nano-PACR has minimal effects. Nano-ABOA and Nano-BBGA show the least reduction in displacements, indicating they are less effective. Overall, nanoparticles contribute to making gypsum harder to bend and more resistant to bending, with the best mechanical performance observed at concentrations of 20% and 30%.

Finding the optimal concentrations of nanoparticles is crucial to prevent agglomeration, maintain their benefits, and ensure material stability. Each nanoparticle, such as Nano-DBB, Nano-ADGR, Nano-PACR, Nano-ABOA, and Nano-

BBGA, improves the mechanical properties and stress distribution of reinforced beams in unique ways. The tangential stress distribution shows a parabolic pattern across the beam's thickness, peaking at the neutral axis (h=0) and extending to -h/2 and h/2.

Future studies should focus on determining the best amounts of Nano-BBGA and Nano-DBB to improve gypsum's mechanical properties while balancing other key properties like shear resistance. Investigating more types of bio-based nano-inclusions could lead to better materials and more effective plaster applications, expanding its use across various industries. Long-term studies are essential to assess the durability and real-world performance of nano-enhanced gypsum, ensuring the benefits observed in lab conditions are replicated in practical applications. Furthermore, it is crucial to explore the optimal concentrations and combinations of nanoparticles to improve performance while maintaining cost-effectiveness. Developing new nanoparticles or hybrid formulations could enhance reinforcement technologies, leading to better beam reinforcement and overall structural improvements.

Nano-DBB has proven to be the most effective nanoparticle for improving gypsum, even at lower concentrations like 10%, offering superior mechanical properties compared to the other nanoparticles tested. Nano-ADGR and Nano-PACR also improve performance but are less effective at reducing deflection and enhancing overall material strength than Nano-DBB. This demonstrates the importance of selecting the right type and quantity of nanoparticles to achieve the desired results. Optimizing the use of nano-bio materials in beam reinforcement can improve stress distribution and mechanical properties, making construction materials last longer and perform better. This also supports more sustainable and efficient building practices.

References

Agrawal, Y. K., & Tandon, S. G. (1971). N-Arylhydroxamic acids. Journal of Chemical & Engineering Data, 16(4), 495–496. https://doi.org/10.1021/je60051a004.

BENFRID, A., & BOUIADJRA, M. B. (2025). A new approach for studying plaster beam bending based on DISS Algerian (nano-short-bio-fibres). Modern Journal of Health and Applied Sciences, 2(1), 43-58. https://orcid.org/0009-0008-4814-6187

Benfrid, A., Benbakhti, A., Harrat, Z. R., Chatbi, M., Krour, B., Bouiadjra, M. B. "Thermomechanical Analysis of Glass Powder Based Eco-concrete Panels: Limitations and Performance Evaluation", Periodica Polytechnica Civil Engineering, 67(4), pp. 1284–1297, 2023. https://doi.org/10.3311/PPci.22781

Benkabou, R., Abbès, B., Abbès, F., Asroun, A., & Li, Y. (2017). Contribution of 3D numerical simulation of instrumented indentation testing in the identification of elastic-viscoplastic behaviour law of a high-performance concrete. Matériaux & Techniques, 105, 102.https://doi.org/10.1051/mattech/2017023

Chatbi, M., Krour, B., Benatta, M. A., Harrat, Z. R., Amziane, S., & Bouiadjra, M. B. (2022). Bending analysis of nano-SiO2 reinforced concrete slabs resting on elastic foundation. Structural Engineering and Mechanics, An Int'l Journal, 84(5), 685-697. https://doi.org/10.12989/sem.2022.84.5.685. https://doi.org/10.12989/sem.2022.84.5.685

Currey, J. D. (2012). The structure and mechanics of bone. Journal of Materials Science, 47,41-54.https://doi.org/10.1007/s10853-011-5914-9 Ghavami, K. (1995). Ultimate load behaviour of bamboo-reinforced lightweight concrete beams. Cement and concrete composites, 17(4), 281-288. https://doi.org/10.1016/0958-9465(95)00018-8

Ebanda, B., Boris, N., & Ateba, A. (2018). Study of the diffusion behavior of water vapor sorption in natural fiber: Rhecktophyllum camerunense. Indian J. Eng., 143-150. Vol. 15, 2018 , 2319–7757 ISSN EISSN 2319–7765, https://www.discoveryjournals.org/

Ghumare, S. M., & Sayyad, A. S. (2017). A new fifth-order shear and normal deformation theory for static bending and elastic buckling of P-FGM beams. Latin American Journal of Solids and Structures, 14, 1893-1911. https://doi.org/10.1590/1679-78253972

Hadji, Lazreg, Daouadji, T. Hassaine, & Bedia, E. Adda. (2015). A refined exponential shear deformation theory for free vibration of FGM beam with porosities. Geomechanics and Engineering, 9(3), 361–372. https://doi.org/10.12989/GAE.2015.9.3.361

Harrat, Z. R., Amziane, S., Krour, B., & Bouiadjra, M. B. (2021). On the static behavior of nano Si0 2 based concrete beams resting on an elastic foundation. Computers and Concrete, 27(6), 575-583. https://doi.org/10.12989/cac.2021.27.6.575

Janssen, J. J. (2000). Designing and building with bamboo (pp. 130-133). Netherlands: International Network for Bamboo and Rattan. International Network for Bamboo and Rattan 2000 . ISBN 81-86247-46-7

Kecir, A., Chatbi, M., Harrat, Z. R., Bachir Bouiadjra, M., Bouremana, M., Krour, B. "Enhancing the Mechanical Performance of Concrete Slabs through the Incorporation of Nano-sized Iron Oxide Particles (Fe2O3): Non-local Bending Analysis", Periodica Polytechnica Civil Engineering, 68(3),pp.842–858, 2024.https://doi.org/10.3311/PPci.23016

Lakkad, S. C., & Patel, J. M. (1981). Mechanical properties of bamboo, a natural composite. Fibre science and technology, 14(4), 319-322. https://doi.org/10.1016/0015-0568(81)90023-3

Mbei, E. G. L., Atangana, A., Bakoura, M., & Nzengwa, R. (2015). Contribution à la caractérisation ultrasonore en vue de la détection du gondolement des fibres dans un matériau composite plâtre/fibres de Rhectophyllum Camerunense. Afrique Science: Revue Internationale des Sciences et Technologie, 11(3), 1-9. ISSN 1813-548X,http://www.afriquescience.info

Molari, L., Coppolino, F. S., & García, J. J. (2021). Arundo donax: A widespread plant with great potential as sustainable structural material. Construction and Building Materials, 268, 121143. https://doi.org/10.1016/j.conbuildmat.2020.121143

Mori, T., & Tanaka, K. (1973). Average stress in matrix and average elastic energy of materials with misfitting inclusions. Acta metallurgica, 21(5), 571-574. https://doi.org/10.1016/0001-6160(73)90064-3

Mourad, C., Rebai, B., Mansouri, K., Khadraoui, F., Berkia, A., & Messas, T. (2024). Investigating the influence of material composition on bending analysis of functionally graded beams using a 2D refined theory. Journal of Computational Applied Mechanics, 55(1), 62-76. https://doi.org/10.22059/jcamech.2024.368866.909

NEYA, B., DUCHEMIN, B., BIZET, L., KANEMA, J. M., & PANTET, A. (2018). Elaboration et caractérisation d'un matériau de construction à base de fibres d'Hibiscus cannabinus L.(Kénaf) et de plâtre. Afrique SCIENCE, 14(1), 96-105.ISSN 1813-548X, http://www.afriquescience.info

Nguyen, D. D., Dao, S. D., Nguyen, X. T., & Giap, V. T. (2025). Stochastic Finite Element Analysis for Static Bending Beams with a Two-Dimensional Random Field of Material Properties. Modelling, 6(2), 37. https://doi.org/10.3390/modelling6020037

Noutegomo, B., Ebanda, F. B., & Atangana, A. (2024). Numerical modelling of hygro-mechanical behavior of Rhecktophyllum Camerunense vegatable fibers. International Journal for Simulation and Multidisciplinary Design Optimization, 15, 18. https://doi.org/10.1051/smdo/2024017

Powała, K., Obraniak, A., Heim, D. "Mechanical Properties of Gypsum-PCM Composite Refined with the Acrylic Copolymer", Periodica Polytechnica Civil Engineering, 66(1), pp. 235–243, 2022. https://doi.org/10.3311/PPci.18135

Reilly, D. T., & Burstein, A. H. (1975). The elastic and ultimate properties of compact bone tissue. Journal of biomechanics, 8(6), 393-405. https://doi.org/10.1016/0021-9290(75)90075-5 Rho, J. Y., Tsui, T. Y., & Pharr, G. M. (1997). Elastic properties of human cortical and trabecular lamellar bone measured by nanoindentation. Biomaterials, 18(20), 1325-1330. https://doi.org/10.1016/S0142-9612(97)00073-2

Yalçin, O. U., & Kaya, A. İ. (2022). Properties of gypsum particleboard with added mineral dolomite. Maderas. Ciencia y tecnología, 24. http://dx.doi.org/10.4067/s0718-221x2022000100428